

Received June 9, 2021, accepted July 8, 2021, date of publication July 13, 2021, date of current version July 23, 2021.

Digital Object Identifier 10.1109/ACCESS.2021.3096969

A Low Profile, Dual-Band, Dual-Polarized Patch Antenna With Antenna-Filter Functions and Its Application in MIMO Systems

JINHAI LIU¹, HANPING LIU¹, XIANGHUA DOU¹, YANKE TANG¹, CHEN ZHANG¹,
LI WANG¹, RONGXIA TANG¹, AND YINGZENG YIN^{1,2}

¹College of Physics and Electronic Information, Dezhou University, Dezhou, Shandong 253023, China

²National Key Laboratory of Antennas and Microwave Technology, Xidian University, Xi'an, Shaanxi 710071, China

Corresponding author: Jinhai Liu (liujinhai568@126.com)

This work was supported in part by the Scientific Research Foundation of Dezhou University under Grant 2019xgrc45, in part by the Science and Technology Development Project of Dezhou under Grant 2019dzkj17, in part by the National Natural Science Foundation of China under Grant U1931106, in part by the Shandong Provincial Natural Science Foundation of China under Grant ZR2019YQ03, and in part by the Project of Shandong QingChuang Science and Technology Plan under Grant 2019KJJ006.

ABSTRACT In this paper, a low profile, dual-band dual-polarized patch antenna is proposed for antenna-filter function with a relatively low profile of 0.032 wavelength. A simple symmetric open/short-circuited stub (O/SCS) is proposed to excite a square radiating patch, and an additional resonant mode is generated except for the patch-mode. At the lower band, the proposed antenna works as a dual-polarized patch antenna. At the upper band, transmission characteristic is obtained between the two ports, and the antenna structure can be used as a bandpass filter. A 1×2 array is also designed to validate its application potential in MIMO system. The two antennas can operate as radiators with high port isolation levels at the lower band. Meanwhile, at the upper band, the two antenna elements can act as one bandpass filter as the good transmission characteristic. In addition, a 2×2 array is also developed meet dual-function demands in dual-polarized MIMO systems. The low profile, simple structures and excellent performances indicate that the proposed antenna can be a good candidate in future wireless communication applications with shared functions.

INDEX TERMS Dual-band antenna, dual-polarized antenna, dual-function, filter, MIMO-application.

I. INTRODUCTION

With the rapid development of wireless communication technologies, more challenges have emerged as the electromagnetic environments get increasingly complicated. Antennas, as one of the most important components in wireless communication system, have been given more functions, such as beam scanning [1], [2], gain-filtering [3]–[7], function-reconfigurable [8], [9], and so on. As the space for antennas in wireless devices become more compact, some other functions are needed in consideration of equipment structure or multi-function integration [10]–[15]. For example, in [10] and [11], two heatsink antennas are proposed as the structures of two antennas are designed to diverge heat easily. In [12] and [13], glass dielectric resonators are investigated to operate as radiators as well as light covers. In [14], a cylindrical

dielectric resonator is used as an antenna. At the same time, the dielectric resonator also works as the load of the wideband phase delay line for impedance matching and phase shifting. In [15], a solid rectangular dielectric resonator is utilized as the antenna, oscillator load, and packaging cover, which gives the radiator more potential functions.

In recent years, with the trend of high integration for wireless devices, antennas tend to be involved in some functions of RF circuits, such as filter functions [16]–[20]. For example, in [16], the proposed cylindrical dielectric resonator antenna can also be used as a filter, and the operating frequency of antenna and filter can be designed independently. In [17], the feedlines of four MIMO antenna element ports help realize beamforming functions. Besides, the four feedlines can also be regarded as a fourth-order bandpass filter, and the channel isolation is higher than 23.6 dB. In [18], a multi-band MIMO microwave and millimeter antenna system is proposed. A tapered slot structure is introduced to work both

The associate editor coordinating the review of this manuscript and approving it for publication was Abhishek K. Jha.

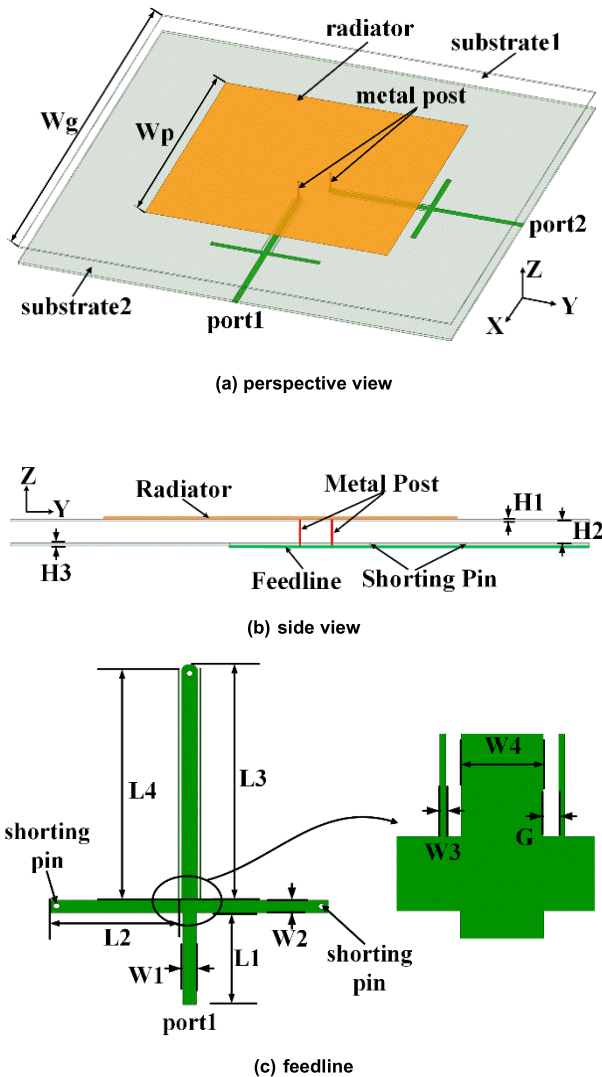


FIGURE 1. Configuration of the proposed antenna: (a) perspective view, (b) side view, (c) microstrip feedline. The optimized parameters are listed as follows (unit: mm): $W_g = 165.0$, $W_p = 89.6$, $W_1 = 2.14$, $W_2 = 2.3$, $W_3 = 0.14$, $W_4 = 1.9$, $L_1 = 33.0$, $L_2 = 18.2$, $L_3 = 36.8$, $L_4 = 36.2$, $G = 0.4$, $H_1 = 0.5$, $H_2 = 0.8$, $H_3 = 6.0$.

as a decoupling structure at microwave frequency band and a slot antenna at millimeter wave band. A dual-polarized magnetolectric dipole is proposed in [19]. By introducing a hook-shaped feedline, a radiation null is generated at the upper band edge, and the selectivity of the antenna is improved. Meanwhile, a bandpass filtering response is obtained at higher frequency band, which is excited by the feedline and magnetolectric dipole.

In the above designs, however, the filter functions are determined by the structures of antennas, and the design principles are complicated. Besides, the filter function of antennas has not been reported in MIMO systems yet. Based on this, a square patch antenna fed by two simple open/short circuited stubs(O/SCS) is proposed in this paper. The antenna performs two resonant bands. It acts as a radiator at the lower frequency band while a bandpass filter at the upper band.

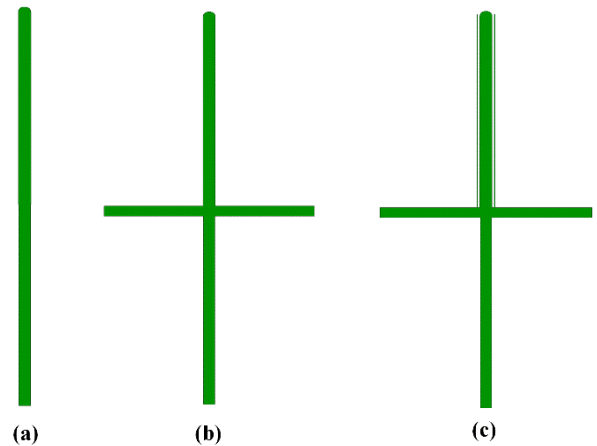


FIGURE 2. Evolution process of the proposed antenna: feedlines of the three antennas: (a) Ant.1, (b) Ant.2, (c) Ant.3(the proposed antenna).

Besides, the performance of the antenna element in 1×2 and 2×2 MIMO applications is also discussed. At last, the antenna element and array are fabricated and measured to validate the design principle. The details are listed in the following sections.

II. ANTENNA ELEMENT AND ANALYSIS

A. ANTENNA CONFIGURATION

The configuration of the antenna element is shown in Fig. 1. The antenna consists of two substrates. The radiating patch is printed on the top layer of substrate1, and the microstrip feedlines are printed on the bottom layer of substrate2. Two vertical metal posts are used to connect the feedlines with the radiator. Each microstrip feedline has a pair of symmetric open/short circuited stubs(O/SCS). The overall height of the element is 0.032 wavelength, which indicates a very low profile. Besides, the structure of the proposed antenna is simple and easy for fabrication.

B. DESIGN PROCESS OF ANTENNA ELEMENT

An evolution process is shown in Fig. 2 to explain the operation principal of the proposed antenna. As can be seen, Ant.1 is a conventional square patch antenna fed by normal microstrip lines. Ant.2 is a pair of symmetrical short-circuited stubs added to Ant.1. Ant.3(the proposed antenna) is a pair of symmetrical open-circuited stubs added to Ant.2. The simulated S-parameters for the three antennas are illustrated in Fig. 3. Ant.1 operates at 1.4 GHz with only one resonant frequency. However, with the introduction of symmetrical short-circuited stubs, another resonant frequency occurs. More importantly, the $|S_{21}|$ for Ant.2 reaches -5.8 dB at the additional frequency point, which indicates a promising transmission characteristic. To get better transmission characteristic, symmetrical open-circuited stubs are added. As a result, the two operating frequencies are separated. At the lower band, the antenna operates at 1.32 GHz. Besides, excellent transmission characteristic for Ant.3 is obtained at

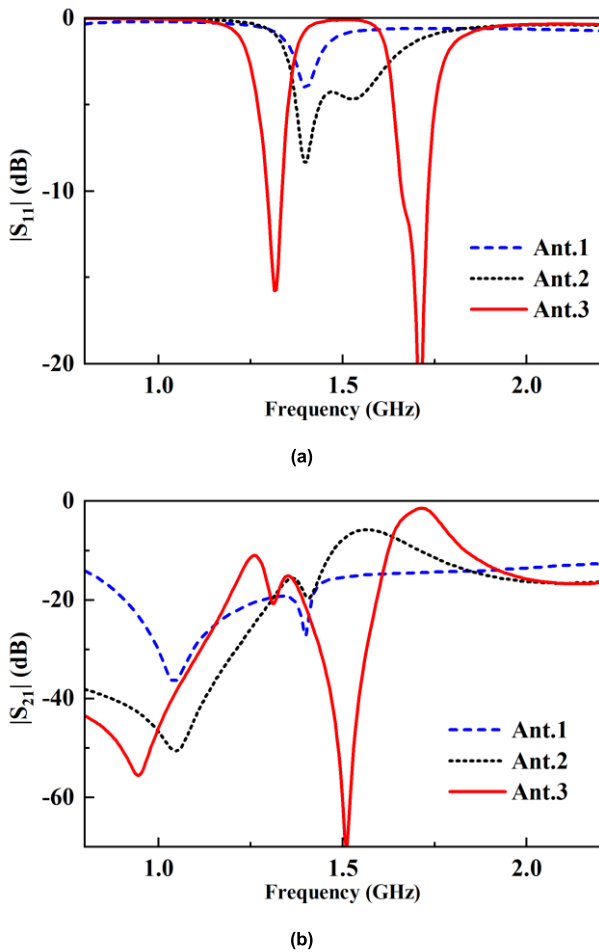


FIGURE 3. Simulated S-parameters for the three antennas: (a) $|S_{11}|$, (b) $|S_{21}|$.

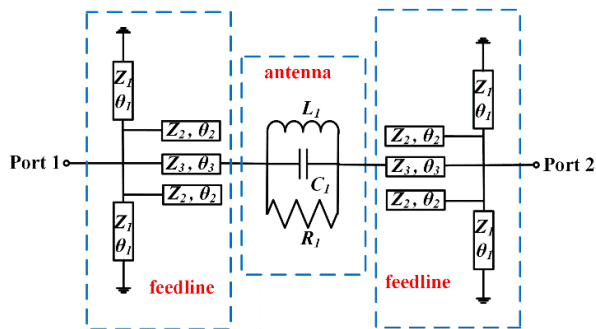


FIGURE 4. Equivalent circuit model for Ant.3.

the upper band, which indicates a good filtering response. Fig. 4 shows the equivalent circuit for Ant.3. It can be seen that the two feedlines are connected directly to the antenna, which means that the transmission characteristic at the upper band is mainly determined by Z_3, θ_3, L_1, C_1 and R_1 . On the other hand, the resonant frequency at the lower band is mainly determined by the antenna structure. Besides, the transmission zero is mainly due to the introduction of open-circuited stub (Z_2, θ_2).

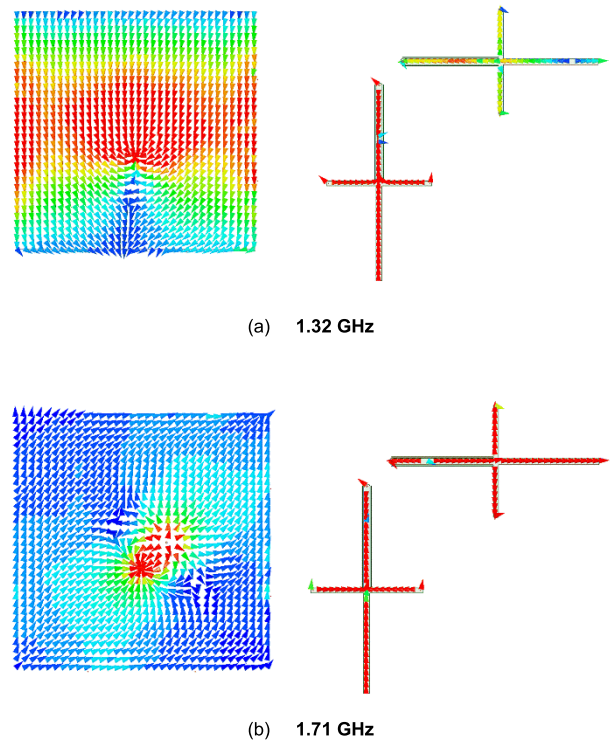


FIGURE 5. Current distributions on the patch and feedlines at (a) 1.32 GHz and (b) 1.71 GHz.

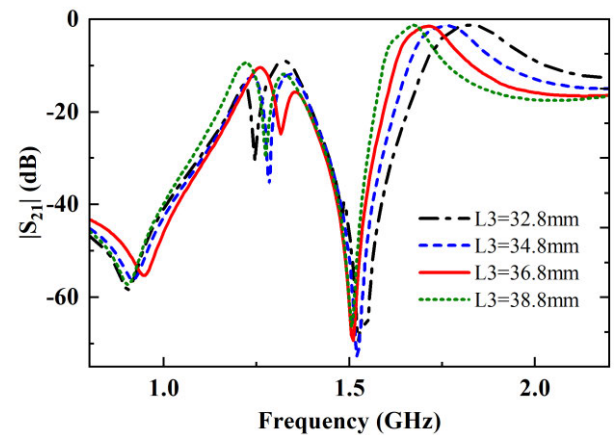


FIGURE 6. Simulated S-parameter varied with L_3 .

Fig. 5 shows the current distributions of the proposed antenna at the two frequencies. At the lower band, current on the patch is about 0.5 wavelength when one port is excited. Besides, currents on the other feedline are weak, which indicates a good port isolation. In addition, currents on the patch are weak at the upper band, except for the section that connecting the two feedlines. At the same time, current on the other feedline is strong, which indicates excellent transmission characteristic between the two ports.

To validate the resonant characteristics of the proposed antenna, some key parameters are studied for better understanding of the working principle. Fig. 6 shows the

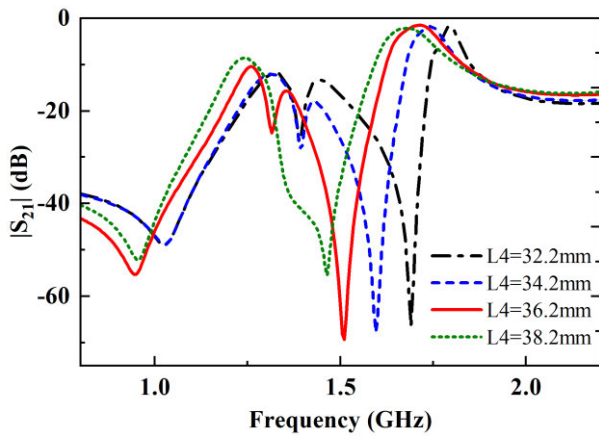


FIGURE 7. Simulated S-parameter varied with L4.

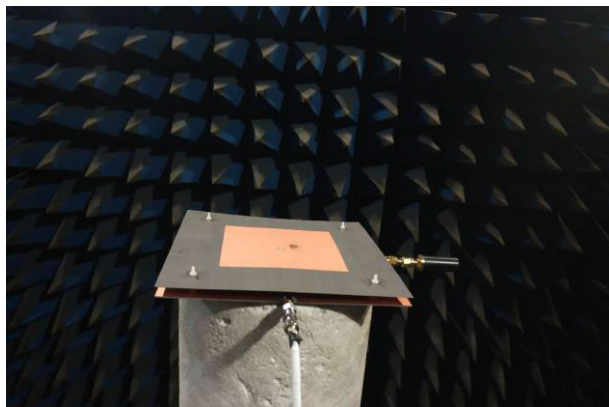


FIGURE 8. Prototype of the proposed antenna element.

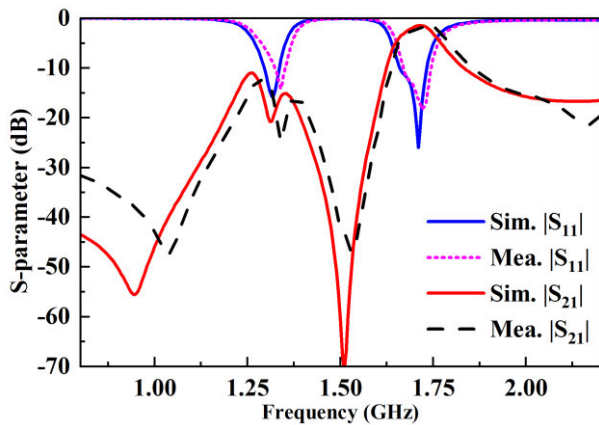


FIGURE 9. Simulated and measured S-parameters for the proposed antenna.

S-parameter varied with L3. It can be seen that the transmission characteristic is greatly influenced by the length of feedline. The resonant frequency moves to lower frequency band as L3 increases, and the transmission null between the two bands keeps steady at the same time. Fig. 7 shows the transmission characteristic varied with length of the open-circuited stub, and the transmission null moves to lower frequency

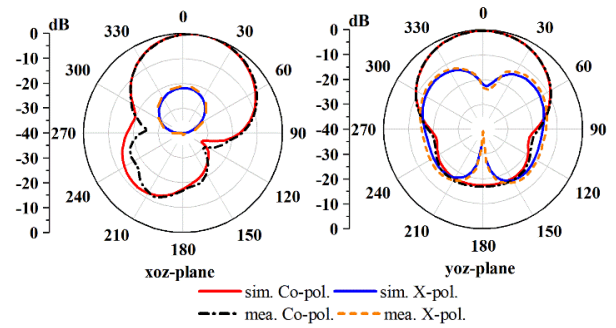


FIGURE 10. Simulated and measured radiation patterns for the proposed antenna at 1.32 GHz.

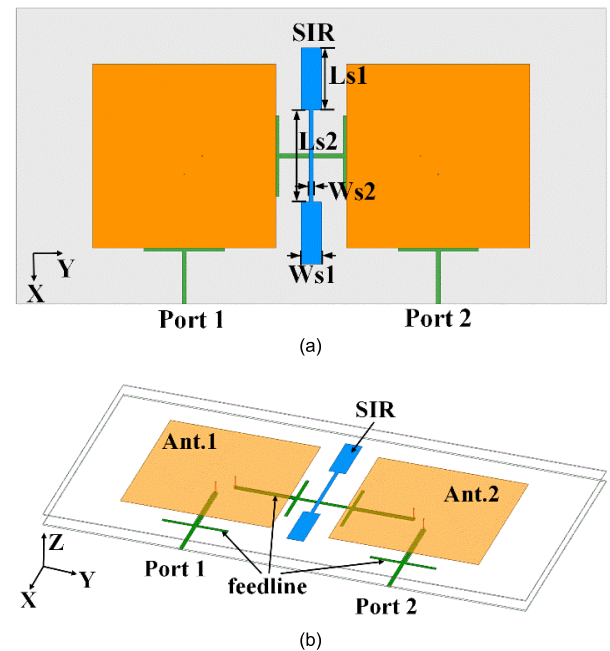


FIGURE 11. Configuration of the proposed 1 × 2 array: (a) top view and (b) 3-D perspective view.

band as L4 increases. As the separation of the two operation bands is mainly due to the introduction of the open-circuited stub, the transmission characteristic at upper band is also influenced by L4. In addition, as the open-circuited stub is close to the feedline (Z_3, θ_3), the capacitance coupling effect between them gets stronger as L4 increases, thus the resonant frequency moves to lower frequency band.

A prototype of the antenna element is fabricated and measured to validate the design, as Fig. 8 shows. The measured S-parameters and the radiation patterns are shown in Fig. 9 and Fig. 10. Good agreements can be found between the measured results and the simulated ones. The measured results show that the proposed antenna element operates from 1.32 GHz to 1.35 GHz for $|S_{11}| < -10$ dB as a radiator, and 1.68 GHz to 1.74 GHz as a bandpass filter. The isolation between the two ports is higher than 18.2dB at lower band, and the measured insertion loss is 1.7 ± 0.5 dB. The insertion loss is mainly produced by material, feedline

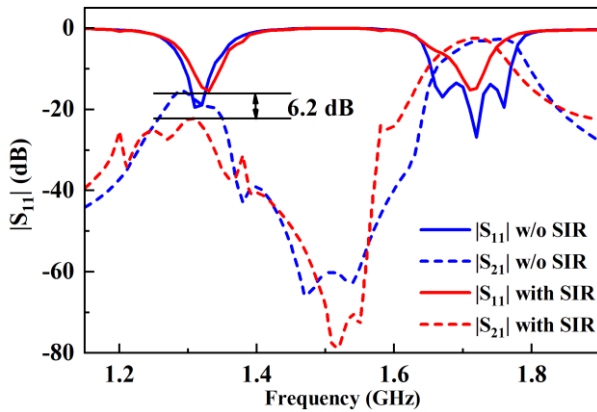


FIGURE 12. Simulated S-parameters for the antenna array with and without SIR.

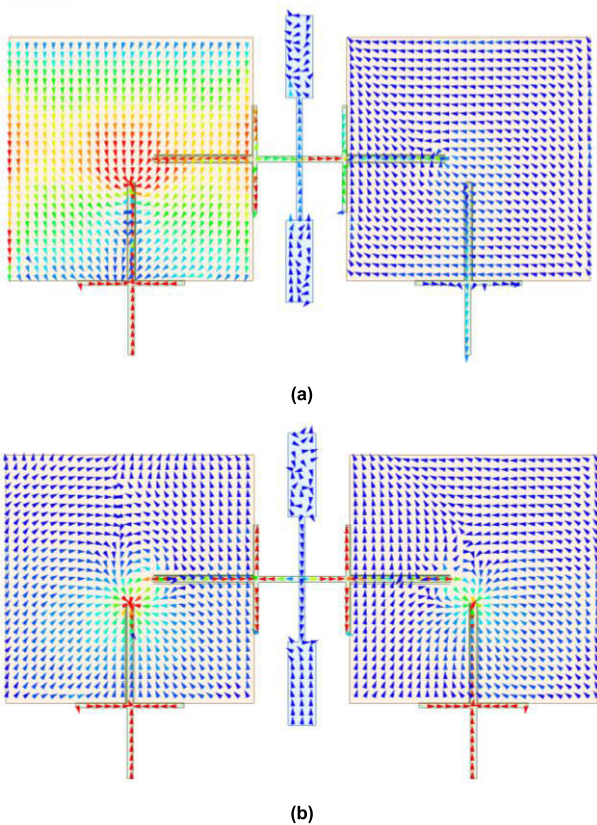


FIGURE 13. Current distributions for the antennas at (a) 1.33GHz and (b) 1.71 GHz.

and measurement. Besides, the antenna element performs unidirectional radiation patterns with peak gain of 8.8 dBi and cross-polarization level of better than 21.9 dB when it acts as an antenna.

III. 1 × 2 ARRAY WITH DUAL-FUNCTION

Fig. 11 shows the configuration of the proposed 1 × 2 array. The antenna element is the same with the one in Section II. Two feedlines are united together to connect the two patches, leaving the other two ports with the same polarization.

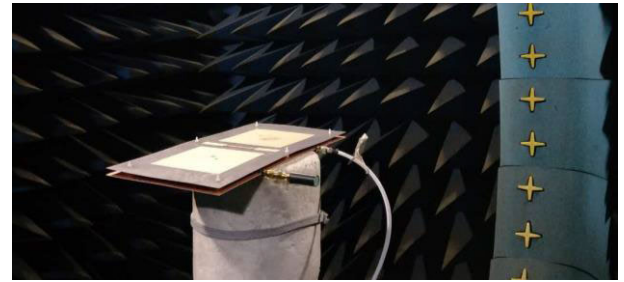


FIGURE 14. Prototype and test environment of the proposed 1 × 2 array.

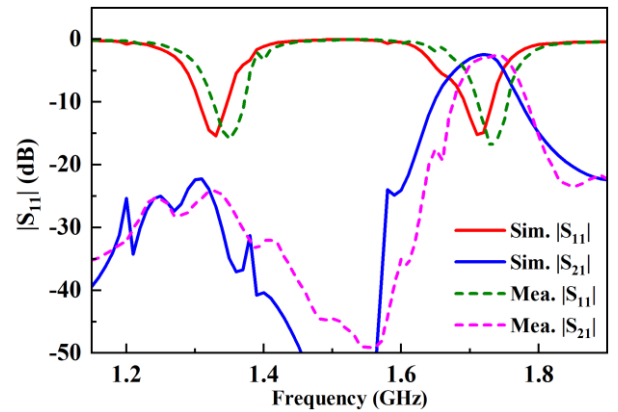


FIGURE 15. Simulated and measured S-parameters for the 1 × 2 array.

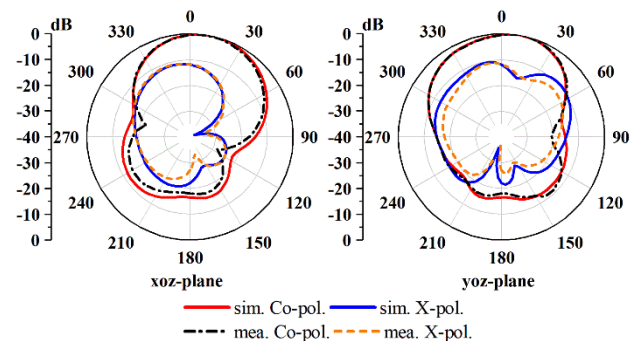


FIGURE 16. Simulated and measured radiation patterns for the 1 × 2 array at 1.35 GHz.

A symmetric stepped-impedance resonator (SIR) is also printed on the top of the upper substrate to suppress the coupling effect between the two antennas. The optimized parameters for the SIR are as follows: $Ls1 = 30.2$, $Ls2 = 45.0$, $Ws1 = 10.0$, $Ws2 = 2.0$ (unit: mm). The distance between the two antenna elements is 34.5mm (0.15 wavelength at the center of lower band). Fig. 12 shows the simulated S-parameters of the antenna array with/ without the SIR. At the lower band, the proposed array can act as two antenna elements with same polarization as the high port isolation levels. At the upper band, however, the proposed array can act as a filter as the transmission characteristic is excellent between the two ports. With the introduction of SIR, the isolation level at lower band is suppressed by 6.2 dB.

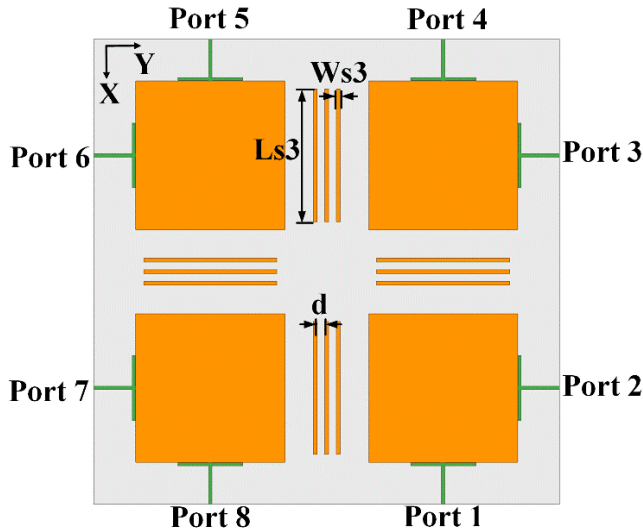


FIGURE 17. Configuration of the proposed 2×2 array. The optimized parameters for the metal strips are as follows: $Ls3 = 80.2$, $Ws3 = 2.2$, $d = 4.9$ (unit: mm).

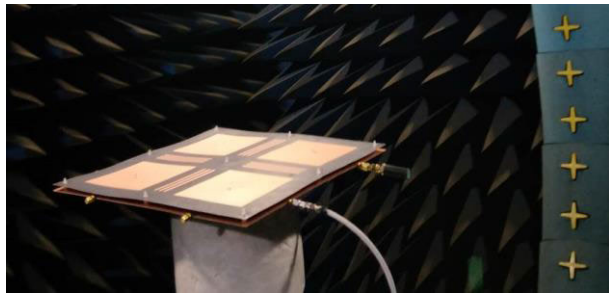
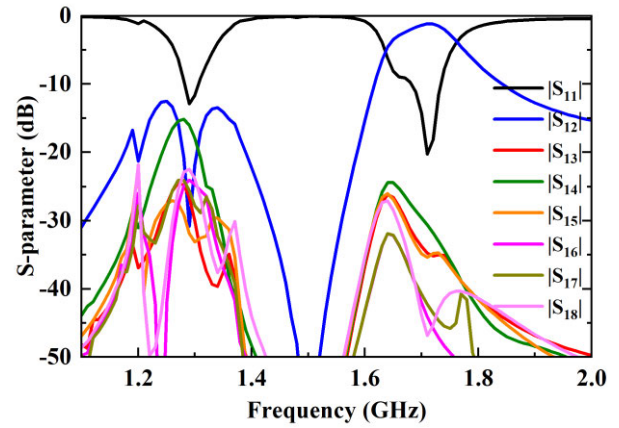


FIGURE 18. Prototype and test environment of the proposed 2×2 array.

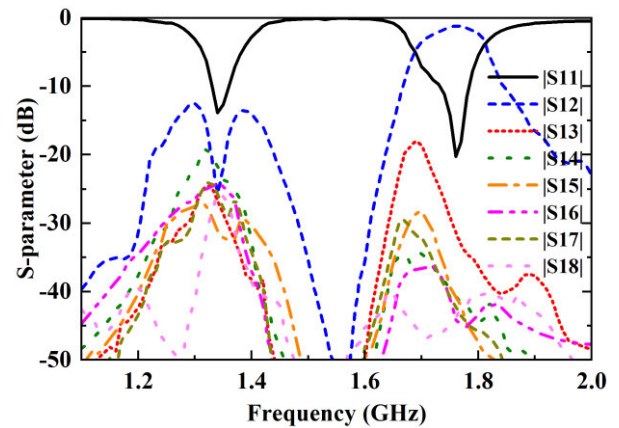
For better view of the working mechanism of the proposed antenna array, current distributions for the array are illustrated in Fig. 13. It can be seen that the transmission characteristic is poor between the two ports at the lower band when port 1 is excited. Meanwhile, current distributions on Ant.1 is about half-wavelength. At the upper band, however, strong currents can be observed on the feedlines, and currents on the two radiators are very weak, which indicates good transmission characteristic. To validate the design principle, a prototype of the 1×2 array is fabricated, as Fig. 14 shows. the measured S-parameters for the array are illustrated in Fig. 15. The array operates from 1.33 GHz to 1.37 GHz for $|S_{11}| < -10$ dB as a radiator, and 1.72 GHz to 1.75 GHz as a bandpass filter. The isolation level between the two ports at lower band is high than 24.2 dB, and he measured insertion loss at upper band is 2.4 ± 0.2 dB. Fig. 16 illustrates the measured radiation patterns at 1.35 GHz when port 1 is excited. Unidirectional radiation patterns with peak gain of 8.0 dBi are also obtained.

IV. 2×2 ARRAY WITH DUAL-FUNCTION

A 2×2 array is also developed to meet the demand for dual-polarized applications, as Fig. 17 and Fig. 20 shows. To suppress the coupling effect between antennas, metal



(a)



(b)

FIGURE 19. (a) Simulated and (b) measured S-parameters for the 2×2 array.

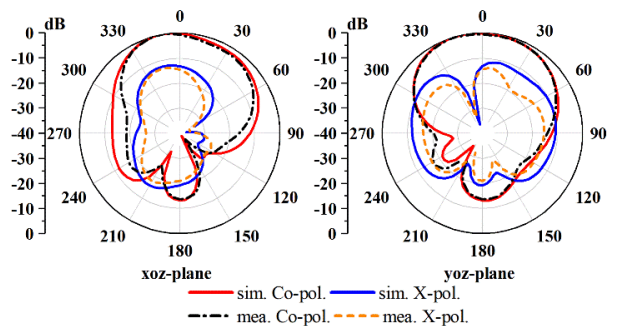


FIGURE 20. Simulated and measured radiation patterns for the 2×2 array at 1.29 GHz.

strips are introduced on the top of the upper substrate. Measured and simulated S-parameters when port 1 is excited are illustrated in Fig. 19. The antenna array operates at 1.33 GHz to 1.36 GHz for $|S_{11}| < -10$ dB as a radiator, and 1.74 GHz to 1.78 GHz as a bandpass filter. Isolation levels between port 1 and the other ports at lower band are all higher than 20.2 dB. At upper band, the measured insertion loss between port 1 and port 2 is 1.4 ± 0.3 dB. Besides, the isolation levels between

port 1 and port 3–port 8 are higher than 26.6 dB. Fig. 20 illustrates the measured radiation patterns when port 1 is excited. Unidirectional radiation patterns are also generated with peak gain of 7.9 dBi at lower band.

V. CONCLUSION

In this paper, a dual-band dual-polarized patch antenna with antenna/filter-function is proposed. As the introduction of open/short-circuited stubs, two operation bands are obtained. At the lower band, the antenna acts as a radiator. At the upper band, the transmission characteristic is excellent between the two ports, and the antenna structure can act as a filter. Besides, the proposed antenna has a very low profile of 0.032 wavelength, as well as a simple structure. In addition, a 1×2 array is also developed with same polarization to validate the potential applications in MIMO systems. At lower band, the two antennas can operate as radiators with high port isolation levels. At upper band, the two antenna elements can act as a bandpass filter as the good transmission characteristic. Besides, a 2×2 array is designed to meet dual-polarized applications in MIMO systems. Excellent performances show that the proposed antenna can be a good candidate in future wireless communication applications with multiple functions.

REFERENCES

- [1] C.-X. Mao, S. Gao, and Y. Wang, "Broadband high-gain beam-scanning antenna array for millimeter-wave applications," *IEEE Trans. Antennas Propag.*, vol. 65, no. 9, pp. 4864–4868, Sep. 2017.
- [2] C. M. K. T. Al-Nuaimi, A. Mahmoud, W. Hong, and Y. He, "Design of single-layer circularly polarized reflectarray with efficient beam scanning," *IEEE Antennas Wireless Propag. Lett.*, vol. 19, no. 6, pp. 1002–1006, Jun. 2020.
- [3] C.-X. Mao, S. Gao, Y. Wang, Q. Luo, and Q.-X. Chu, "A shared-aperture dual-band dual-polarized filtering-antenna-array with improved frequency response," *IEEE Trans. Antennas Propag.*, vol. 65, no. 4, pp. 1836–1844, Apr. 2017.
- [4] X. Y. Zhang, Y. Zhang, Y.-M. Pan, and W. Duan, "Low-profile dual-band filtering patch antenna and its application to LTE MIMO system," *IEEE Trans. Antennas Propag.*, vol. 65, no. 1, pp. 103–113, Jan. 2017.
- [5] Y. Li, Z. Zhao, Z. Tang, and Y. Yin, "Differentially fed, dual-band dual-polarized filtering antenna with high selectivity for 5G sub-6 GHz base station applications," *IEEE Trans. Antennas Propag.*, vol. 68, no. 4, pp. 3231–3236, Apr. 2020.
- [6] Y. Li, Z. Zhao, Z. Tang, and Y. Yin, "Differentially-fed, wideband dual-polarized filtering antenna with novel feeding structure for 5G sub-6 GHz base station applications," *IEEE Access*, vol. 7, pp. 184718–184725, 2019.
- [7] L.-H. Wen, S. Gao, Q. Luo, Z. Tang, W. Hu, Y. Yin, Y. Geng, and Z. Cheng, "A balanced feed filtering antenna with novel coupling structure for low-sidelobe radar applications," *IEEE Access*, vol. 6, pp. 77169–77178, 2018.
- [8] Y. Liu, P. Liu, Z. Meng, L. Wang, and Y. Li, "A planar printed non-band loop-monopole reconfigurable antenna for mobile handsets," *IEEE Antennas Wireless Propag. Lett.*, vol. 17, no. 8, pp. 1575–1579, Aug. 2018.
- [9] P.-Y. Qin, Y. J. Guo, Y. Cai, E. Dutkiewicz, and C.-H. Liang, "A reconfigurable antenna with frequency and polarization agility," *IEEE Antennas Wireless Propag. Lett.*, vol. 10, pp. 1373–1376, 2011.
- [10] J. J. Casanova, J. A. Taylor, and J. Lin, "Design of a 3-D fractal heatsink antenna," *IEEE Antennas Wireless Propag. Lett.*, vol. 9, pp. 1061–1064, 2010.
- [11] L. Covert and J. Lin, "Simulation and measurement of a heatsink antenna: A dual-function structure," *IEEE Trans. Antennas Propag.*, vol. 54, no. 4, pp. 1342–1349, Apr. 2006.
- [12] K. W. Leung, Y. M. Pan, X. S. Fang, E. H. Lim, K.-M. Luk, and H. P. Chan, "Dual-function radiating glass for antennas and light covers—Part I: Omnidirectional glass dielectric resonator antennas," *IEEE Trans. Antennas Propag.*, vol. 61, no. 2, pp. 578–586, Feb. 2013.
- [13] K. W. Leung, X. S. Fang, Y. M. Pan, E. H. Lim, K. M. Luk, and H. P. Chan, "Dual-function radiating glass for antennas and light covers—Part II: Dual-band glass dielectric resonator antennas," *IEEE Trans. Antennas Propag.*, vol. 61, no. 2, pp. 587–597, Feb. 2013.
- [14] Y.-X. Sun, K. W. Leung, and J.-F. Mao, "Dual function dielectric resonator antenna and phase-delay-line load: Designs of compact circularly polarized/differential antennas," *IEEE Trans. Antennas Propag.*, vol. 66, no. 1, pp. 414–419, Jan. 2018.
- [15] E. H. Lim and K. W. Leung, "Novel utilization of the dielectric resonator antenna as an oscillator load," *IEEE Trans. Antennas Propag.*, vol. 55, no. 10, pp. 2686–2691, Oct. 2007.
- [16] E. H. Lim and K. W. Leung, "Use of the dielectric resonator antenna as a filter element," *IEEE Trans. Antennas Propag.*, vol. 56, no. 1, pp. 5–10, Jan. 2008.
- [17] Y. Zhang, X. Y. Zhang, and Q. H. Liu, "A six-port dual-function RF device with four-element MIMO antenna array and bandpass filter operations," *IEEE Trans. Antennas Propag.*, vol. 68, no. 6, pp. 4549–4559, Jun. 2020.
- [18] M. Ikram, N. Nguyen-Trong, and A. Abbosh, "Multiband MIMO microwave and millimeter antenna system employing dual-function tapered slot structure," *IEEE Trans. Antennas Propag.*, vol. 67, no. 8, pp. 5705–5710, Aug. 2019.
- [19] Y. Zhang, X. Y. Zhang, L. Gao, Y. Gao, and Q. H. Liu, "A two-port microwave component with dual-polarized filtering antenna and single-band bandpass filter operations," *IEEE Trans. Antennas Propag.*, vol. 67, no. 8, pp. 5590–5601, Aug. 2019.
- [20] J.-Y. Lin, S.-W. Wong, L. Zhu, Y. Yang, X. Zhu, Z.-M. Xie, and Y. He, "A dual-functional triple-mode cavity resonator with the integration of filters and antennas," *IEEE Trans. Antennas Propag.*, vol. 66, no. 5, pp. 2589–2593, May 2018.



JINHAI LIU received the Ph.D. degree from Xidian University, Xi'an, China, in 2018. Since 2018, he has been a Lecturer with Dezhou University, Dezhou, China. His research interests include multiband antenna, UWB antennas, phased array antennas, and high gain antennas for base stations.



HANPING LIU received the Ph.D. degree in optical engineering from Shandong University, Jinan, China, in 2008. He is currently an Associate Professor with the College of Physics and Electronic Information, Dezhou University, Dezhou, China. He has published more than ten research articles in refereed international journals and conferences, such as *Journal of Physics D* and *Chinese Physics Letters*. His research interests include wireless sensors, radio frequency identification, and the Internet of Things technology.



XIANGHUA DOU received the B.S. degree from Qufu University, Qufu, China, in 1993. He is currently an Associate Professor with Dezhou University. His research interests include radio frequency identification, computer aided design for antennas, and the Internet of Things technology.



YANKE TANG received the Ph.D. degree in physics from the University of Chinese Academy of Sciences, in 2008. He is currently a Professor with the College of Physics and Electronic Information, Dezhou University. His research interests include radio telescope antennas and the Internet of Things technology.



CHEN ZHANG received the B.S. and M.S. degrees in electrical engineering from Hebei Polytechnic University, Tangshan, Hebei, China, in 2001 and 2004, respectively. She is currently a Lecturer with the College of Physics and Electronic Information, Dezhou University, Dezhou, China. Her research interests include filtering antenna, wideband antenna, and circular polarized antenna.



LI WANG received the B.S. degree from Yantai Normal University, in 2003, and the M.S. degree from the University of Electronic Science and Technology of China, in 2006. She is currently a Lecturer with the College of Physics and Electronic Information, Dezhou University, Dezhou, China. Her research interests include filter and radio frequency identification.



RONGXIA TANG received the M.S. degree in communication and information system from Shandong University, Jinan, China, in 2009. She is currently a Lecturer with the College of Physics and Electronic Information, Dezhou University. Her research interests include filtering antenna, computer aided design for antennas, and radio frequency identification.



YINGZENG YIN received the B.S., M.S., and Ph.D. degrees in electromagnetic wave and microwave technology from Xidian University, Xi'an, China, in 1987, 1990, and 2002, respectively. From 1990 to 1992, he was a Research Assistant and an Instructor with the Institute of Antennas and Electromagnetic Scattering, Xidian University, where he was an Associate Professor with the Department of Electromagnetic Engineering, from 1992 to 1996, and has been a Professor, since 2004. His current research interests include the design of micro strip antennas, feeds for parabolic reflectors, artificial magnetic conductors, phased array antennas, and base-station antennas.

...